Thin-Section MR Imaging for Carotid Cavernous Fistula

D. Kim, Y.J. Choi, Y. Song, S.R. Chung, J.H. Baek, and J.H. Lee

ABSTRACT

BACKGROUND AND PURPOSE: Carotid-cavernous fistulas are abnormal vascular shunts that can cause various neurologic or orbital symptoms. The purpose of this retrospective study was to evaluate the diagnostic performance of thin-section MR imaging for carotid cavernous fistula in patients with clinically suspected carotid cavernous fistula, and to identify possible imaging predictors of carotid cavernous fistula.

MATERIALS AND METHODS: A total of 98 patients who were clinically suspected of having carotid cavernous fistula (according to their symptoms and physical examinations) between January 2006 and September 2018 were included in this study. The patients underwent pretreatment thin-section MR imaging and DSA. Thin-section MR imaging consisted of 2D coronal T1- and T2WI with 3-mm thickness and 3D contrast-enhanced T1WI with 0.6 mm thickness. The diagnostic performance of thin-section MR imaging for carotid cavernous fistula was evaluated with the reference standard of DSA. Univariate logistic regression analysis was performed to determine possible imaging predictors of carotid cavernous fistula.

RESULTS: Among the 98 patients, DSA confirmed 38 as having carotid cavernous fistula. The overall accuracy, sensitivity, and specificity of thin-section MR imaging were 88.8%, 97.4%, and 83.3%, respectively. Possible imaging predictors on thin-section MR imaging included abnormal contour of the cavernous sinus (OR: 21.7), internal signal void of the cavernous sinus (OR: 15.3), prominent venous drainage flow (OR: 54.0), and orbital/periorbital soft tissue swelling (OR: 40.4).

CONCLUSIONS: Thin-section MR imaging provides high diagnostic performance and possible imaging predictors of carotid cavernous fistula in patients with clinically suspected carotid cavernous fistula. Thin-section MR imaging protocols could help decide appropriate management plans for patients with clinically suspected carotid cavernous fistula.

ABBREVIATION: CCF = carotid cavernous fistula

Carotid cavernous fistulas (CCFs) are abnormal vascular shunts connecting the carotid artery and cavernous sinus. The flow can originate either directly from the cavernous segment of the internal carotid artery (direct CCF), or indirectly through dural branches from the internal carotid artery or external carotid artery (indirect CCF or cavernous sinus dural arteriovenous fistula).[1] Common clinical symptoms of CCF include proptosis, conjunctival injection, chemosis, diplopia, headaches, subjective bruit, visual disturbance, and ocular pain.[2-5] The reference standard for the diagnosis and classification of CCF is DSA, which is also essential for management planning.[6,7] However, DSA is not routinely performed in all patients with suspected symptoms because of its semi-invasiveness. So, after consideration of clinical symptoms and imaging findings of CT, CTA, MR imaging, or MRA, physicians decide whether to perform DSA. DSA also presents limitations in the evaluation of structures other than vessels, such as orbital soft tissue and brain parenchyma.

CT, CTA, MR imaging, or MRA are usually used as the initial imaging technique for CCF.[8] The imaging findings on CT include proptosis, dilated superior ophthalmic veins, enlargement of extraocular muscles, orbital and periorbital soft tissue swelling, and focal bulging or diffuse distention of the cavernous sinus. Most CT findings are also visible on MR imaging.[9-18] Additionally, an abnormal signal void within the cavernous sinus due to increased flow may also be visible in patients with

Received March 10, 2020; accepted after revision May 26.

From the Department of Radiology and Research Institute of Radiology (D.K., Y.J.C., Y.S., S.R.C., J.H.B., J.H.L.), Asan Medical Center, University of Ulsan College of Medicine, Seoul, Republic of Korea; and Department of Radiology (D.K.), Busan Paik Hospital, Inje University College of Medicine, Busan, Republic of Korea.

Please address correspondence to Young Jun Choi, MD, PhD, Associate Professor, Department of Radiology and Research Institute of Radiology, University of Ulsan College of Medicine, Asan Medical Center, 86 Asanbyeongwon-gil, Songpa-gu, Seoul, 05505, Republic of Korea; e-mail: jehee23@gmail.com

Indicates article with supplemental on-line table.

http://dx.doi.org/10.3174/ajnr.A6757

CCF, though some studies described considerable numbers of false-positive and false-negative cases for this finding.[10,13] On MRA or CTA, visualization of flow signal or early contrast enhancement within the cavernous sinuses along with dilated draining veins can also be helpful for screening or diagnosing CCF.[19-24] Three-dimensional TOF MRA is known to be very sensitive in detecting CCF with some downside in the specificity.[19,22,25] More recent techniques to visualize CCF include 4D-CTA and arterial spin-labeled MR imaging.[26,27] With advances in MR imaging techniques, the resolution of MR imaging has notably increased over time and continues to do so. In head and neck imaging specifically, the fine structures of the cranial nerves and vascular anatomy have become more vivid owing to the introduction of thin-section MR imaging.[28-30] Due to its complex anatomy and relatively small size, the cavernous sinus is better depicted on thin-section MR imaging.[31] Additionally, subtle change of contour or signal change of cavernous sinus might be easily depicted on thin-section MR imaging. In the clinical setting, certain types of thin-section MR imaging for evaluating cranial nerve and orbit, are frequently used as the initial imaging technique for patients with orbital or cranial nerve symptoms. To the best of our knowledge, there is no published research on the diagnostic performance of thin-section MR imaging for CCF. Therefore, the purpose of our study was to evaluate the usefulness of thin-section MR imaging on a large cohort of patients with clinically suspected CCF.

MATERIALS AND METHODS

This retrospective study was approved by the review boards of our institution, and the requirement for informed consent for data evaluation was waived. The methods and reporting of the results are in accordance with the STROBE (Strengthening the Reporting of Observational Studies in Epidemiology) statement.[32] There was no external financial support for this study.

Study Population

The study population was obtained from a historical cohort of consecutive patients with clinically suspected CCF according to their symptoms and physical examinations, and who underwent pretreatment thin-section MR imaging and DSA between January 2006 and September 2018 at Asan Medical Center (2700 beds), an academic tertiary referral hospital in Seoul, Korea. The patients' symptoms included diplopia, eyeball pain, facial pain, ptosis, proptosis, periorbital swelling, eyeball injection, and visual disturbance. Patients were excluded from the study population if 1) they were under the age of 18, 2) the interval between thin-section MR imaging and DSA was more than 90 days, 3) thin-section MR imaging or DSA were obtained after treatment, and 4) the thin-section MR imaging or DSA image quality was poor. The patient selection procedure is summarized in Fig 1. Finally, 98 patients (32 men and 66 women) were enrolled. The age range of the patients was from 20 to 85 years, with a mean age of 54.6 years (standard deviation: 14.6 years).

Imaging Protocols

All patients underwent pretreatment thin-section MR imaging and DSA for evaluation of CCF. Because of the long study period, various MR imaging and DSA systems were used; however, most MR examinations were performed with a 3-T MR unit (Intera Achieva; Philips Medical Systems) by using a 16-element phased-array head coil. Two-dimensional coronal T1-weighted, T2-weighted (with and without fat suppression), and contrast-enhanced T1-weighted turbo spin-echo images were obtained at a 3-mm thickness. Contrast-enhanced 3D T1-turbo field echo images were obtained with a 0.6-mm thickness and reconstruction section thickness was 1.2 mm with an interslice distance of 0.6-mm. The scan range of the coronal and axial images covered the orbit and cavernous sinus. Detailed parameters for the thin-section MR imaging are summarized in On-line Table. Cerebral DSA images included both internal carotid arteriograms, both external carotid arteriograms, and both vertebral arteriograms.

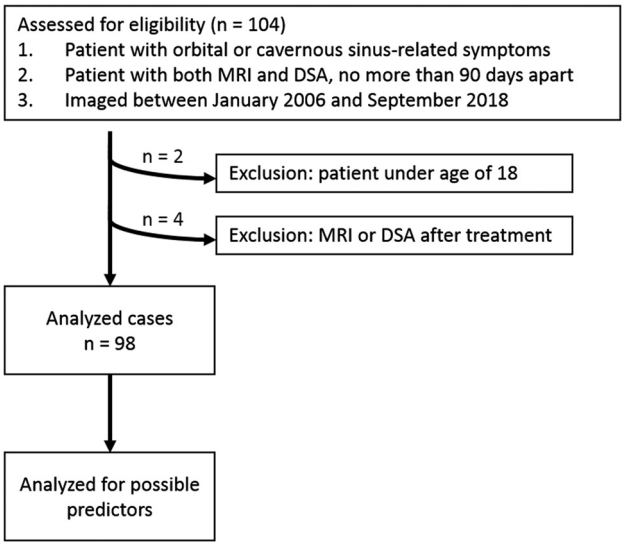

FIG 1. Flow diagram of the case selection procedure and case numbers in each subgroup.

Interpretation of Images

The thin-section MRIs of all patients were interpreted in consensus by 2 neuroradiologists (D.K. and Y.J.C., with 5 and 13 years of clinical experience in neuroradiology, respectively). Before evaluation, the 2 neuroradiologists completed a training session on imaging from 5 patients to help them reach a consensus on evaluation of the imaging findings. The 2 neuroradiologists were blinded to other radiologic imaging including the DSA, and to clinical information including symptoms, signs, and treatment given to the patients. The following possible imaging predictors for CCF on pretreatment thin-section MR imaging were analyzed: 1) abnormal contour of the cavernous sinus, 2) abnormal internal signal void of the cavernous sinus, 3) prominent venous drainage flow (anterior/lateral/posterior), and 4) orbital/periorbital soft tissue swelling.

Abnormal contour of the cavernous sinus was considered positive if the cavernous sinus was asymmetrically enlarged and the lateral wall of the cavernous sinus was outwardly convex or straight on the coronal view (Fig 2). Abnormal internal signal void of the cavernous sinus was considered positive if there was a signal void larger than 2 mm in the shortest diameter within or along the wall of the cavernous sinus on coronal imaging (Fig 3).

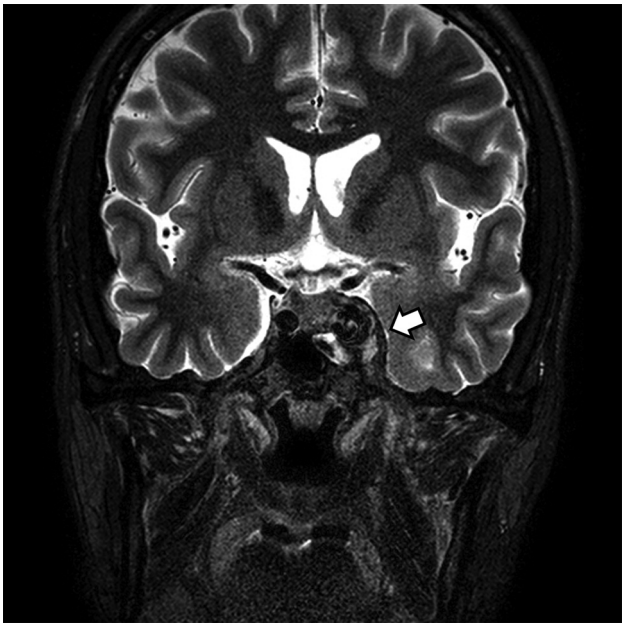

FIG 2. A CCF case with abnormal contour of the cavernous sinus. Coronal T2-weighted image of a patient with diplopia, confirmed to be left sixth cranial nerve palsy on neurologic examination. Note the abnormal contour bulging of the left cavernous sinus (*arrow*). An internal signal void was also noted on both T2-weighted (*arrow*) and T1-weighted imaging (not shown). The patient was confirmed as having a direct CCF on digital subtraction angiography.

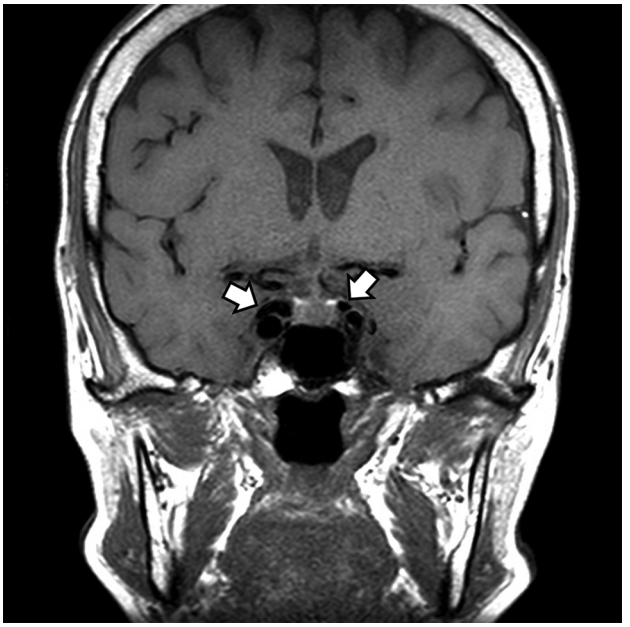

FIG 3. A CCF case with internal signal void of the cavernous sinuses. Coronal T1-weighted image of a patient with diplopia, confirmed to be right third cranial nerve palsy on neurologic examination. Note the internal signal void in both cavernous sinuses visible on T1-weighted image (*arrows*). The patient was confirmed to have an indirect CCF on digital subtraction angiography.

Signal void was evaluated on both T1- and T2-weighted MR imaging. Prominent venous drainage flow was considered positive if the superior or inferior ophthalmic vein (anterior), sphenoparietal sinus (lateral), or superior or inferior petrosal sinus (posterior) was prominently or asymmetrically enlarged with or without signal void (Figs 4 and 5). Orbital/periorbital soft tissue swelling was considered positive if there was high signal change and extraocular muscle thickening on T2-weighted MR imaging (Fig 6). The overall diagnosis (presence or absence of CCF) was also evaluated for each case, and the diagnostic performance of thin-section MR imaging was estimated.

The DSAs of all patients were reviewed by a neurointervention-dedicated neuroradiologist (Y.S, with 5 years of clinical experience in neuroradiology). The neuroradiologist was blinded to other radiologic images, including the thin-section MR imaging, and to clinical information, including symptoms and signs of the patient and treatment performed. The presence or absence of CCF on DSA was evaluated and considered as the reference standard. When present, the type of CCF (whether direct or indirect) was also evaluated. For patients with indirect CCF, a further classification according to Suh et al[33] (proliferative type, having numerous arterial feeders to the cavernous sinus; restrictive type, showing many delineable arterial feeders converging to the cavernous sinus; or late restrictive type, showing a few arterial feeders with sluggish retrograde venous flow) was determined.

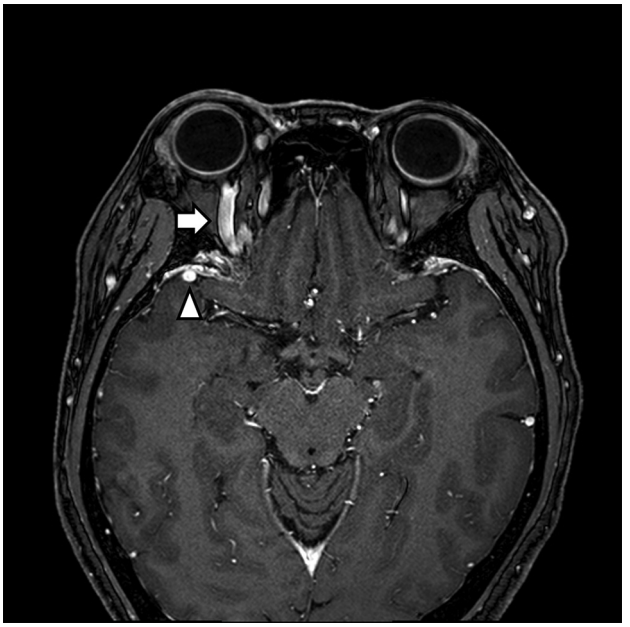

FIG 4. A CCF case with prominent venous drainage flow in the anterior and lateral venous structures. Axial contrast-enhanced T1-weighted image of a patient with right ocular pain and conjunctival injection. Note the enlarged right superior ophthalmic vein (anterior; *arrow*) and right sphenoparietal sinus (lateral; *arrowhead*). The patient was confirmed as having an indirect CCF on digital subtraction angiography.

Statistical Analysis

This study had 2 main outcomes. The primary outcome was the diagnostic performance of thin-section MR imaging for the diagnosis of CCF with the reference standard being DSA. The sensitivity, specificity, accuracy, positive and negative predictive values, and appropriate use criteria of the receiver operating characteristic curves of thin-section MR imaging for depicting the

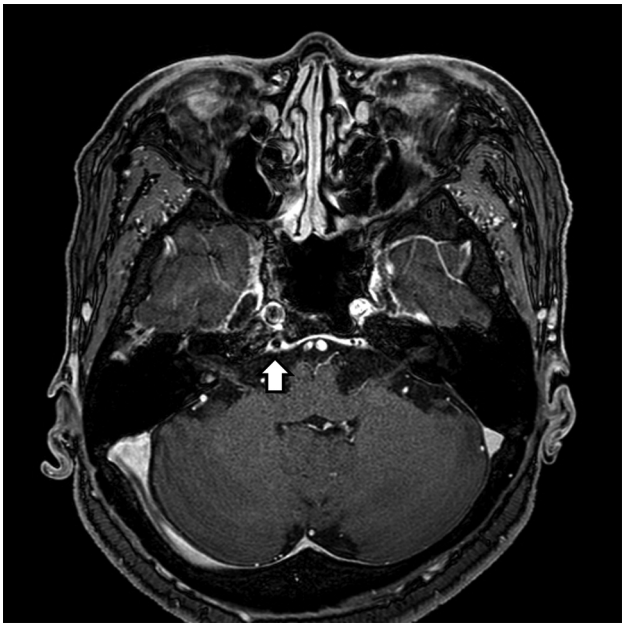

FIG 5. A CCF case with prominent venous drainage flow in the posterior venous structure. Axial contrast-enhanced T1-weighted image of a patient with diplopia, confirmed to be right sixth cranial nerve palsy on neurologic examination. Note the enlarged right inferior petrosal sinus (posterior) with an internal signal void (*arrow*) indicating increased flow rate. The patient was confirmed as having an indirect CCF on digital subtraction angiography.

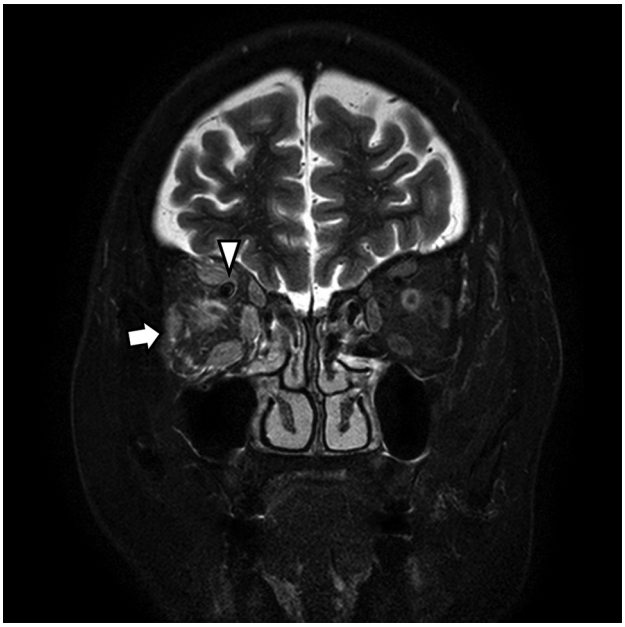

FIG 6. A CCF case with high signal change and orbital soft tissue thickening. Coronal T2-weighted image of a patient with periorbital swelling, conjunctival injection, ocular pain, and diplopia. Fat stranding and swelling of extraocular muscles (*arrow*) are noted. Prominent venous drainage flow in the superior ophthalmic vein is also noted (*arrowhead*). The patient was confirmed as having an indirect CCF on digital subtraction angiography.

presence of CCF were calculated. The secondary outcome was to determine possible imaging predictors for CCF on thin-section MR imaging. The Fisher exact test and univariable logistic regression analysis were used to determine possible predictors of CCF. The thin-section MR imaging characteristics of abnormal contour of the cavernous sinus, internal signal void of the cavernous sinus, prominent venous drainage flow (anterior/lateral/posterior), and orbital/periorbital soft tissue swelling were considered as potential adjustment variables. Statistical analyses were performed by using SPSS software (version 25.0; IBM), with statistical significance being defined as $P < .05$.

RESULTS

Among the 98 patients, 38 were confirmed as having CCF on DSA. Six patients had direct CCF, and 32 patients had indirect CCF. The baseline characteristics and clinical manifestations of the patients are summarized in Table 1. The overall diagnostic performance of thin-section MR imaging for diagnosing CCF was as follows: accuracy, sensitivity, and specificity were 88.8%, 97.4%, and 83.3%, respectively. There was 1 false-negative case (3.1%, 1/38) on thin-section MR imaging. Among the 32 indirect CCF cases, there were 10 proliferative type cases, 17 restrictive type cases, and 5 late restrictive type cases, while the single false-negative case was a late restrictive type. Among the 60 patients confirmed as CCF-negative on DSA, there were 10 false-positive cases on thin-section MR imaging (16.7%, 10/60).

In the univariable logistic regression, patients with CCF showed higher odds of an abnormal contour of the cavernous sinus (OR: 21.7), internal signal void of the cavernous sinus (OR: 15.3), prominent venous drainage flow in anterior, lateral, or posterior drainage venous structures (OR: 54.0), and orbital/periorbital soft tissue swelling (OR: 40.4) on thin-section MR imaging. The results of the univariable logistic regression are summarized in Table 2.

Radiologists do not usually rely on a single imaging feature to diagnose a disease; therefore, we analyzed various combinations of features to determine the best ones for diagnosis. Among the various feature combinations showing an accuracy above 85%, "any prominent venous drainage flow" and "internal signal void of the cavernous sinus" (combination 1) showed the highest accuracy (91.8%); "any prominent venous drainage flow" (anterior/lateral/posterior) and "orbital/periorbital soft tissue swelling" (combination 2) showed the highest specificity (96.7%) and positive likelihood ratio (23.7); and "prominent anterior venous drainage flow" or "orbital/periorbital soft tissue swelling" (combination 3) showed the highest sensitivity (92.1%) and the lowest negative likelihood ratio (0.097). The diagnostic performances of each feature and combination of features are summarized in Table 3.

DISCUSSION

In this study, we analyzed the diagnostic performance of thin-section MR imaging for CCF, and determined possible thin-section MR imaging predictors for CCF, by using a historical cohort of patients with clinically suspected CCF. The accuracy, sensitivity, and specificity of thin-section MR imaging for diagnosis of CCF were 88.8%, 97.4%, and 83.3%,

respectively. Patients with CCF showed a higher prevalence of abnormal contour of the cavernous sinus (OR: 21.7), internal signal void of the cavernous sinus (OR: 15.3), prominent venous drainage flow (OR: 54.0), and orbital/periorbital soft tissue swelling (OR: 40.4) on thin-section MR imaging.

Most of the research focusing on the MR imaging findings of CCF was conducted between the late 1980s and early 1990s.[9-13] The MR imaging findings of these studies included low or dark signal within the cavernous sinus, dilated superior ophthalmic vein, swelling of the extraocular muscles, and bulging of the lateral wall of the cavernous sinus. Uchino et al[12] analyzed 10 cases of indirect CCF and found that 9 out of 10 cases (90%) were positive for flow void within the cavernous sinus, and 8 out of 10 cases (80%) were positive for dilated superior ophthalmic vein on MR imaging. These findings correlate well with the results of our study, in which 92.1% of the CCF cases showed internal signal void within the cavernous sinus, and 78.9% showed prominent anterior venous drainage flow. However, most previous research covers case series studies in which the number of cases was less than or equal to 10. The study protocols used in previous studies mainly included non-3D T1-weighted, T2-weighted, and postcontrast T1-weighted imaging with section thickness ranging from 2 to 10 mm, acquired on scanners with magnetic fields equal to or less than 1.5T. To our knowledge, there has been no study on the diagnostic performance of MR imaging for CCF that has included a large number of cases. There was 1 false-negative case on thin-section MR imaging, which was an indirect CCF (late restrictive type). The late restrictive type CCF is characterized by a few arterial feeders and sluggish retrograde venous flow on DSA,[33] and these hemodynamic characteristics may be the cause for the incorrect diagnosis on thin-section MR imaging. There were 10 false-positive cases (16.7%) in terms of overall diagnostic performance in our study. In the false-positives, the common image findings were signal void in the cavernous sinus (10 cases), abnormal contour of cavernous sinus (9 cases), and prominent venous drainage flow in the lateral (4 cases) and posterior (4 cases) venous drainage structures. In most of our study cases, where fistulous or venous flow was not very slow, thin-section MR imaging showed satisfactory diagnostic performance in patients with clinically suspected CCF, with especially high sensitivity. Our study also focused on evaluating the possible imaging predictors for CCF on thin-section MR imaging. Abnormal contour of the cavernous sinus (OR: 21.7), internal signal void of the cavernous sinus (OR: 15.3), prominent venous drainage flow in anterior, lateral, or posterior drainage venous structures (OR: 54.0), and orbital/periorbital soft tissue swelling (OR: 40.4) on thin-section MR imaging were shown to be possible imaging predictors for CCF on thin-section MR imaging. Abnormal contour and signal void of the cavernous sinus were visible on coronal T1WI and T2WI with 3-mm thickness. Prominent venous drainage flows were best seen on the contrast-enhanced 3D T1WI with 0.6 mm thickness and axial reconstruction. Orbital/periorbital soft tissue swelling was well visualized on coronal images with 3-mm thickness, whereas it was not clearly visualized on contrast-enhanced 3D T1WI. It is evident that thin-section MR imaging is helpful in searching for these fine struc-

Table 1: Clinical characteristics of the study patients

	All Patients (n = 98)	CCF Positive Patients (n = 38)	CCF Negative Patients (n = 60)
Sex, *n*			
Male/Female	32/66	11/27	21/39
Age, years			
Mean (range)	54.6 (20–85)	66.0 (24–85)	51.4 (20–81)
Symptoms, *n* (%)			
Diplopia	54 (55.1)	20 (52.6)	34 (56.7)
Eyeball pain	27 (27.6)	14 (36.8)	13 (21.7)
Facial pain	2 (2.0)	1 (2.6)	1 (1.7)
Ptosis	30 (30.6)	8 (21.1)	22 (36.7)
Proptosis	14 (14.3)	9 (23.7)	5 (8.3)
Periorbital swelling	19 (19.4)	16 (42.1)	3 (5)
Conjunctival injection	23 (23.5)	16 (42.1)	7 (11.7)
Visual disturbance	18 (18.4)	7 (18.4)	11 (18.3)
Headache	40 (40.8)	14 (36.8)	26 (43.3)
Dizziness	13 (13.3)	5 (13.2)	8 (13.3)
Neurologic signs, *n* (%)			
Laterality			
Right	30 (30.6)	8 (21.1)	22 (36.7)
Left	22 (22.4)	6 (15.8)	16 (26.7)
3rd cranial neve palsy	26 (26.5)	4 (10.5)	22 (36.7)
4th cranial nerve palsy	5 (5.1)	2 (5.3)	3 (5)
6th cranial nerve palsy	22 (22.4)	8 (21.1)	14 (23.3)
Trauma history, *n* (%)	5 (5.1)	3 (7.9)	2 (3.3)

Table 2: Logistic regression of thin-section MR imaging predictors for CCF

Feature	Total	CCF Cases	Univariable Logistic Regression	
			OR (95% CI)	*P* Value
Abnormal contour of cavernous sinus	57.1% (56/98)	92.1% (35/38)	21.7 (6.0–78.9)	<.001
Signal void of cavernous sinus	73.5% (72/98)	92.1% (35/38)	15.3 (4.2–55.1)	<.001
Prominent venous drainage flow[a]	52.0% (51/98)	94.7% (36/38)	54.0 (11.6–251.7)	<.001
Anterior	36.7% (36/98)	78.9% (30/38)	33.8 (10.7–106.5)	<.001
Lateral	22.4% (22/98)	34.2% (13/38)	3.0 (1.1–7.8)	.030
Posterior	23.5% (23/98)	47.4% (18/38)	9.9 (3.3–30.2)	<.001
Orbital/periorbital soft tissue swelling	39.8% (39/98)	84.2% (32/38)	40.4 (12.5–130.8)	<.001

[a] Prominent venous drainage flow indicates the presence of prominent venous drainage flow in at least 1 of the anterior, lateral, and posterior prominent venous drainage flows.

Table 3: Diagnostic performance of each thin-section MR imaging feature and combination of imaging features for CCF[a]

	Accuracy	Sensitivity	Specificity	PLR	NLR
Abnormal contour of cavernous sinus	75.5% (65.8–83.6%)	92.1% (78.6–98.3)	65% (51.6–76.9)	2.6 (1.8–3.8)	0.1 (0.0–0.4)
Signal void of cavernous sinus	70.4% (60.7–78.5%)	92.1% (79.2–97.3)	56.7% (44.1–68.4)	2.1 (1.6–2.9)	0.1 (0.0–0.4)
Any prominent venous drainage flow	82.7% (74.0–88.9)	94.7% (82.7–98.5)	75% (62.8–84.2)	3.8 (2.4–5.9)	0.1 (0.0–0.3)
Prominent anterior venous drainage flow	85.7% (77.4–91.3)	79.0% (63.7–88.9)	90% (79.9–95.3)	7.9 (3.6–7.2)	0.2 (0.1–0.4)
Prominent lateral venous drainage flow	65.3% (55.0–74.6)	34.2% (19.6–51.2)	85% (73.4–92.9)	2.3 (1.1–4.8)	0.8 (0.6–1.0)
Prominent posterior venous drainage flow	74.5% (64.7–82.8)	47.4% (31.0–64.2)	91.7% (81.6–97.2)	5.7 (2.3–14.0)	0.6 (0.4–0.8)
Orbital/periorbital soft tissue swelling	86.7% (78.6–92.1)	84.2% (69.6–92.6)	88.3% (77.8–94.2)	7.2 (3.6–14.7)	0.2 (0.1–0.4)
Combination 1 (any prominent venous drainage flow AND internal signal void of cavernous sinus)	91.8% (84.7–95.8)	89.5% (75.9–95.8)	93.3% (84.1–97.4)	13.4 (5.2–34.8)	0.1 (0.0–0.3)
Combination 2 (any prominent venous drainage flow AND orbital/periorbital soft tissue swelling)	89.8% (82.2–94.4)	79.0% (63.7–88.9)	96.7% (88.6–99.1)	23.7 (6.0–93.4)	0.2 (0.1–0.4)
Combination 3 (prominent anterior venous drainage flow OR orbital/periorbital soft tissue swelling)	85.7% (77.4–91.3)	92.1% (79.2–97.3)	81.7% (70.1–89.4)	5.0 (2.9–8.6)	0.1 (0.0–0.3)

Note:—PLR indicates positive likelihood ratio; NLR, negative likelihood ratio.
[a] Data in parentheses are 95% confidence intervals.

tures and lesions, though determination of the optimal section thickness may require additional study.

There are several limitations to this study. First, the study was retrospective and patients were selected on the basis of their electronic medical records and the presence of certain radiologic examinations. This might have resulted in a selection bias. Furthermore, the MR imaging reviewers were aware that the patients had undergone DSA, and this might have induced some reader bias and might have affected diagnostic performance. Second, because this was a single-center study, the generalizability of these results may be limited, and a further prospective multicenter study may be needed. Third, there was a delay of up to 90 days between the MR imaging and DSA. However, in most cases the delay was less than 30 days (86.7%), and considering the slow-evolving natural course of CCF, this delay may be acceptable. Fourth, the comparison of thin-section MR imaging with CTA or MRA was not conducted. CTA and 3D TOF-MRA are also known as good modalities for screening CCF with high sensitivities. However, the case numbers of concurrent CTA with thin-section MR imaging and 3D TOF-MRA with thin-section MR imaging were too small to perform the comparative analysis in our study. Therefore, the results of this study do not justify the replacement of CTA or MRA to thin-section MR imaging in case of clinically suspected CCF. However, the results may be helpful in differentiating the cause of orbital or cranial nerve symptoms in patients who have undergone the thin-section MR imaging without CTA or MRA.

CONCLUSIONS

Thin-section MR imaging showed high performance for diagnosing CCF in patients with clinically suspected CCF. The possible imaging predictors for CCF on thin-section MR imaging included abnormal contour of the internal signal void in the cavernous sinus; prominent venous flow in the ophthalmic vein, sphenoparietal sinus, or petrosal sinus; and orbital/periorbital soft tissue swelling.

Disclosures: Jung Hwan Baek—*UNRELATED:* Consultancy: Radiofrequency ablation, *Comments:* STARmed and RF medical company from 2017.

REFERENCES

1. Barrow DL, Spector RH, Braun IF, et al. **Classification and treatment of spontaneous carotid-cavernous sinus fistulas.** *J Neurosurg* 1985;62:248–56 CrossRef Medline
2. Henderson AD, Miller NR. **Carotid-cavernous fistula: current concepts in aetiology, investigation, and management.** *Eye (Lond)* 2018;32:164–72 CrossRef Medline
3. Grumann AJ, Boivin-Faure L, Chapot R, et al. **Ophthalmologic outcome of direct and indirect carotid cavernous fistulas.** *Int Ophthalmol* 2012;32:153–59 CrossRef Medline
4. Keizer R. **Carotid-cavernous and orbital arteriovenous fistulas: ocular features, diagnostic and hemodynamic considerations in relation to visual impairment and morbidity.** *Orbit* 2003;22:121–42 CrossRef
5. Lasjaunias P, Chiu M, ter Brugge K, et al. **Neurological manifestations of intracranial dural arteriovenous malformations.** *J Neurosurg* 1986;64:724–30 CrossRef Medline
6. Modic MT, Berlin AJ, Weinstein MA. **The use of digital subtraction angiography in the evaluation of carotid cavernous sinus fistulas.** *Ophthalmology* 1982;89:441–44 CrossRef Medline
7. Debrun GM. **Angiographic workup of a carotid cavernous sinus fistula (CCF) or what information does the interventionalist need for treatment?** *Surg Neurol* 1995;44:75–79 CrossRef Medline
8. Dos Santos D, Monsignore LM, Nakiri GS, et al. **Imaging diagnosis of dural and direct cavernous carotid fistulae.** *Radiology Bras* 2014;47:251–55 CrossRef Medline
9. Hirabuki N, Miura T, Mitomo M, et al. **MR imaging of dural arteriovenous malformations with ocular signs.** *Neuroradiology* 1988;30:390–94 CrossRef Medline
10. Komiyama M, Fu Y, Yagura H, et al. **MR imaging of dural AV fistulas at the cavernous sinus.** *J Comput Assist Tomogr* 1990;14:397–401 CrossRef Medline
11. Elster AD, Chen MY, Richardson DN, et al. **Dilated intercavernous sinuses: an MR sign of carotid-cavernous and carotid-dural fistulas.** *AJNR Am J Neuroradiol* 1991;12:641–45
12. Uchino A, Hasuo K, Matsumoto S, et al. **MRI of dural carotid-cavernous fistulas. Comparisons with postcontrast CT.** *Clin Imaging* 1992;16:263–68 CrossRef Medline
13. Hirabuki N, Fujita N, Hashimoto T, et al. **Follow-up MRI in dural arteriovenous malformations involving the cavernous sinus:**

emphasis on detection of venous thrombosis. *Neuroradiology* 1992; 34:423–27 CrossRef Medline
14. Hirai T, Korogi Y, Hamatake S, et al. **Three-dimensional FISP imaging in the evaluation of carotid cavernous fistula: comparison with contrast-enhanced CT and spin-echo MR.** *AJNR Am J Neuroradiol* 1998;19:253–59
15. Kwon BJ, Han MH, Kang H-S, et al. **MR imaging findings of intracranial dural arteriovenous fistulas: relations with venous drainage patterns.** *AJNR Am J Neuroradiol* 2005;26:2500–07 Medline
16. Merrick R, Latchaw RE, Gold L. **Computerized tomography of the orbit in carotid-cavernous sinus fistulae.** *Comput Tomogr* 1980; 4:127–32 CrossRef Medline
17. Zilkha A, Daiz AS. **Computed tomography in carotid cavernous fistula.** *Surg Neurol* 1980;14:325–29 Medline
18. Ahmadi J, Teal JS, Segall HD, et al. **Computed tomography of carotid-cavernous fistula.** *AJNR Am J Neuroradiol* 1983;4:131–36 Medline
19. Ikawa F, Uozumi T, Kiya K, et al. **Diagnosis of carotid-cavernous fistulas with magnetic resonance angiography—demonstrating the draining veins utilizing 3-D time-of-flight and 3-D phase-contrast techniques.** *Neurosurg Rev* 1996;19:7–12 CrossRef Medline
20. Coskun O, Hamon M, Catroux G, et al. **Carotid-cavernous fistulas: diagnosis with spiral CT angiography.** *AJNR Am J Neuroradiol* 2000;21:712–16 Medline
21. Rucker JC, Biousse V, Newman NJ. **Magnetic resonance angiography source images in carotid cavernous fistulas.** *Br J Ophthalmol* 2004;88:311 CrossRef Medline
22. Chen CCC, Chang PT, Shy CG, et al. **CT angiography and MR angiography in the evaluation of carotid cavernous sinus fistula prior to embolization: a comparison of techniques.** *AJNR Am J Neuroradiol* 2005;26:2349–56
23. Akiba H, Tamakawa M, Hyodoh H, et al. **Assessment of dural arteriovenous fistulas of the cavernous sinuses on 3D dynamic MR angiography.** *AJNR Am J Neuroradiol* 2008;29:1652–57 CrossRef Medline
24. Lee JY, Jung C, Ihn YK, et al. **Multidetector CT angiography in the diagnosis and classification of carotid–cavernous fistula.** *Clinical Radiology* 2016;71:e64–71 CrossRef
25. Ouanounou S, Tomsick TA, Heitsman C, et al. **Cavernous sinus and inferior petrosal sinus flow signal on three-dimensional time-of-flight MR angiography.** *AJNR Am J Neuroradiol* 1999;20:1476–81 Medline
26. van Amerongen MJ, Pegge SAH, El Kandoussi M, et al. **The non-invasive search for the carotid-cavernous fistula: the added value of the 4D-CTA.** *Neuroradiology* 2017;59:835–37 CrossRef Medline
27. Yamamoto N, Yamamoto Y, Izumi Y, et al. **Dural arterivenous fistula at the cavernous sinus diagnosed by arterial spin-labeled imaging.** *Intern Med* 2018;57:1163–66 CrossRef Medline
28. Ettl A, Kramer J, Daxer A, et al. **High resolution magnetic resonance imaging of neurovascular orbital anatomy.** *Ophthalmology* 1997; 104:869–77 CrossRef Medline
29. Tanitame K, Sone T, Kiuchi Y, et al. **Clinical applications of high-resolution ocular magnetic resonance imaging.** *Jpn J Radiology* 2012; 30:695–705 CrossRef Medline
30. Lee JH, Cheng KL, Choi YJ, et al. **High-resolution imaging of neural anatomy and pathology of the neck.** *Korean J Radiology* 2017; 18:180–93 CrossRef Medline
31. Ettl A, Zwrtek K, Daxer A, et al. **Anatomy of the orbital apex and cavernous sinus on high-resolution magnetic resonance images.** *Surv Ophthalmol* 2000;44:303–23 CrossRef Medline
32. von EE, Altman DG, Egger M, et al. **Strengthening the reporting of observational studies in epidemiology (STROBE) statement: guidelines for reporting observational studies.** *BMJ* 2007;335:806–08 CrossRef Medline
33. Suh DC, Lee JH, Kim SJ, et al. **New concept in cavernous sinus dural arteriovenous fistula: correlation with presenting symptom and venous drainage patterns.** *Stroke* 2005;36:1134–39 CrossRef